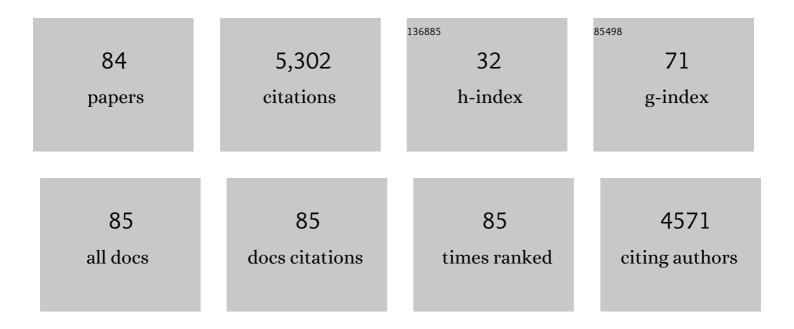
List of Publications by Year in descending order

Source: https://exaly.com/author-pdf/3132780/publications.pdf Version: 2024-02-01



#	Article	IF	CITATIONS
1	A Biomimetic Potassium Responsive Nanochannel: G-Quadruplex DNA Conformational Switching in a Synthetic Nanopore. Journal of the American Chemical Society, 2009, 131, 7800-7805.	6.6	316
2	Adsorptive environmental applications of MXene nanomaterials: a review. RSC Advances, 2018, 8, 19895-19905.	1.7	313
3	Gating of Single Synthetic Nanopores by Proton-Driven DNA Molecular Motors. Journal of the American Chemical Society, 2008, 130, 8345-8350.	6.6	295
4	Enhanced Photocatalytic Removal of Uranium(VI) from Aqueous Solution by Magnetic TiO ₂ /Fe ₃ O ₄ and Its Graphene Composite. Environmental Science & Technology, 2017, 51, 5666-5674.	4.6	292
5	Synthesis of novel nanomaterials and their application in efficient removal of radionuclides. Science China Chemistry, 2019, 62, 933-967.	4.2	256
6	Efficient U(VI) Reduction and Sequestration by Ti ₂ CT _{<i>x</i>} MXene. Environmental Science & Technology, 2018, 52, 10748-10756.	4.6	253
7	Efficient removal of uranium from aqueous solution by zero-valent iron nanoparticle and its graphene composite. Journal of Hazardous Materials, 2015, 290, 26-33.	6.5	231
8	Loading Actinides in Multilayered Structures for Nuclear Waste Treatment: The First Case Study of Uranium Capture with Vanadium Carbide MXene. ACS Applied Materials & Interfaces, 2016, 8, 16396-16403.	4.0	214
9	Rational control of the interlayer space inside two-dimensional titanium carbides for highly efficient uranium removal and imprisonment. Chemical Communications, 2017, 53, 12084-12087.	2.2	198
10	Photocatalytic reduction of uranium(VI) by magnetic ZnFe2O4 under visible light. Applied Catalysis B: Environmental, 2020, 267, 118688.	10.8	170
11	Effective removal of U(VI) and Eu(III) by carboxyl functionalized MXene nanosheets. Journal of Hazardous Materials, 2020, 396, 122731.	6.5	166
12	Effective Removal of Anionic Re(VII) by Surface-Modified Ti ₂ CT _{<i>x</i>} MXene Nanocomposites: Implications for Tc(VII) Sequestration. Environmental Science & Technology, 2019, 53, 3739-3747.	4.6	163
13	Efficient thorium(IV) removal by two-dimensional Ti2CTx MXene from aqueous solution. Chemical Engineering Journal, 2019, 366, 192-199.	6.6	163
14	A reliable and programmable acoustofluidic pump powered by oscillating sharp-edge structures. Lab on A Chip, 2014, 14, 4319-4323.	3.1	152
15	Nanolayered Ti ₃ C ₂ and SrTiO ₃ Composites for Photocatalytic Reduction and Removal of Uranium(VI). ACS Applied Nano Materials, 2019, 2, 2283-2294.	2.4	119
16	Adsorption of uranyl species on hydroxylated titanium carbide nanosheet: A first-principles study. Journal of Hazardous Materials, 2016, 308, 402-410.	6.5	115
17	Aryl Diazonium-Assisted Amidoximation of MXene for Boosting Water Stability and Uranyl Sequestration via Electrochemical Sorption. ACS Applied Materials & Interfaces, 2020, 12, 15579-15587.	4.0	115
18	Highly efficient adsorption and immobilization of U(VI) from aqueous solution by alkalized MXene-supported nanoscale zero-valent iron. Journal of Hazardous Materials, 2021, 408, 124949.	6.5	95

#	Article	IF	CITATIONS
19	Sorption of Eu(III) on MXene-derived titanate structures: The effect of nano-confined space. Chemical Engineering Journal, 2019, 370, 1200-1209.	6.6	91
20	Exploring Actinide Materials Through Synchrotron Radiation Techniques. Advanced Materials, 2014, 26, 7807-7848.	11.1	89
21	Anion-adaptive crystalline cationic material for 99TcO4â^' trapping. Nature Communications, 2019, 10, 1532.	5.8	87
22	How the geometric configuration and the surface charge distribution influence the ionic current rectification in nanopores. Journal Physics D: Applied Physics, 2007, 40, 7077-7084.	1.3	65
23	Photocatalytic reduction of uranium(VI) under visible light with 2D/1D Ti3C2/CdS. Chemical Engineering Journal, 2021, 420, 129831.	6.6	64
24	Electrochemical behaviors of Dy(III) and its co-reduction with Al(III) in molten LiCl-KCl salts. Electrochimica Acta, 2014, 147, 87-95.	2.6	62
25	lon current rectification inversion in conic nanopores: Nonequilibrium ion transport biased by ion selectivity and spatial asymmetry. Journal of Chemical Physics, 2013, 138, 044706.	1.2	58
26	Low-voltage electroosmotic pumps fabricated from track-etched polymer membranes. Lab on A Chip, 2012, 12, 1710.	3.1	53
27	Enhanced photocatalytic reduction of aqueous Re(VII) in ambient air by amorphous TiO2/g-C3N4 photocatalysts: Implications for Tc(VII) elimination. Chemical Engineering Journal, 2020, 401, 125977.	6.6	48
28	Supramolecular inclusion-based molecular integral rigidity: a feasible strategy for controlling the structural connectivity of uranyl polyrotaxane networks. Chemical Communications, 2015, 51, 11990-11993.	2.2	44
29	Layered structure-based materials: challenges and opportunities for radionuclide sequestration. Environmental Science: Nano, 2020, 7, 724-752.	2.2	44
30	Molecular Springâ€like Tripleâ€Helix Coordination Polymers as Dualâ€Stress and Thermally Responsive Crystalline Metal–Organic Materials. Angewandte Chemie - International Edition, 2020, 59, 16061-16068.	7.2	39
31	A facile additive-free method for tunable fabrication of UO2 and U3O8 nanoparticles in aqueous solution. CrystEngComm, 2014, 16, 2645.	1.3	38
32	Halogen Bonded Three-Dimensional Uranyl–Organic Compounds with Unprecedented Halogen–Halogen Interactions and Structure Diversity upon Variation of Halogen Substitution. Crystal Growth and Design, 2015, 15, 1395-1406.	1.4	36
33	In-situ anodic precipitation process for highly efficient separation of aluminum alloys. Nature Communications, 2021, 12, 5777.	5.8	36
34	Surface Modification of Single Track-Etched Nanopores with Surfactant CTAB. Langmuir, 2009, 25, 8870-8874.	1.6	35
35	Efficient Photocatalytic Reduction of Aqueous Perrhenate and Pertechnetate. Environmental Science & Technology, 2019, 53, 10917-10925.	4.6	32
36	Size-dependent toxicity of ThO2 nanoparticles to green algae Chlorella pyrenoidosa. Aquatic Toxicology, 2019, 209, 113-120.	1.9	32

#	Article	IF	CITATIONS
37	Controllable etching of heavy ion tracks with organic solvent addition in etchant. Nuclear Instruments & Methods in Physics Research B, 2008, 266, 3095-3099.	0.6	31
38	Size-tunable synthesis of monodisperse thorium dioxide nanoparticles and their performance on the adsorption of dye molecules. CrystEngComm, 2014, 16, 10469-10475.	1.3	31
39	Thermodynamic and electrochemical properties of holmium and HoxAly intermetallic compounds in the LiCl-KCl eutectic. Electrochimica Acta, 2015, 174, 15-25.	2.6	29
40	Tetranuclear Uranyl Polyrotaxanes: Preferred Selectivity toward Uranyl Tetramer for Stabilizing a Flexible Polyrotaxane Chain Exhibiting Weakened Supramolecular Inclusion. Chemistry - A European Journal, 2015, 21, 10226-10235.	1.7	27
41	Rapid Determination of Uranium in Water Samples by Adsorptive Cathodic Stripping Voltammetry Using a Tin-Bismuth Alloy Electrode. Electrochimica Acta, 2015, 174, 925-932.	2.6	27
42	A method to tune the ionic current rectification of track-etched nanopores by using surfactant. Physical Chemistry Chemical Physics, 2011, 13, 576-581.	1.3	25
43	Copper/Zinc-Directed Heterometallic Uranyl-Organic Polycatenating Frameworks: Synthesis, Characterization, and Anion-Dependent Structural Regulation. Inorganic Chemistry, 2016, 55, 10125-10134.	1.9	23
44	Fabrication and photosensitivity of CdS photoresistor on silica nanopillars substrate. Materials Science in Semiconductor Processing, 2016, 56, 217-221.	1.9	23
45	Application of Binary Ga–Al Alloy Cathode in U Separation from Ce: The Possibility in Pyroprocessing of Spent Nuclear Fuel. Electrochimica Acta, 2020, 353, 136449.	2.6	23
46	First principles modeling of zirconium solution in bulk UO2. Journal of Applied Physics, 2013, 113, .	1.1	22
47	Templateâ€Free Synthesis and Mechanistic Study of Porous Threeâ€Dimensional Hierarchical Uraniumâ€Containing and Uranium Oxide Microspheres. Chemistry - A European Journal, 2014, 20, 12655-12662.	1.7	20
48	New Insight of Coordination and Extraction of Uranium(VI) with N-Donating Ligands in Room Temperature Ionic Liquids: <i>N</i> , <i>N</i> ′-Diethyl- <i>N</i> , <i>N</i> ′-ditolyldipicolinamide as a Case Study. Inorganic Chemistry, 2015, 54, 1992-1999.	1.9	20
49	Easily prepared and stable functionalized magnetic ordered mesoporous silica for efficient uranium extraction. Science China Chemistry, 2016, 59, 629-636.	4.2	20
50	Synthesis of ThO ₂ nanostructures through a hydrothermal approach: influence of hexamethylenetetramine (HMTA) and sodium dodecyl sulfate (SDS). RSC Advances, 2014, 4, 52209-52214.	1.7	19
51	Confirmation and elimination of cyclic electrolysis of uranium ions in molten salts. Electrochemistry Communications, 2019, 103, 55-60.	2.3	19
52	Two Three-Dimensional Actinide-Silver Heterometallic Coordination Polymers Based on 2,2â€2-Bipyridine-3,3â€2-dicarboxylic Acid with Helical Chains Containing Dimeric or Trimeric Motifs. European Journal of Inorganic Chemistry, 2017, 2017, 1472-1477.	1.0	18
53	First three-dimensional actinide polyrotaxane framework mediated by windmill-like six-connected oligomeric uranyl: dual roles of the pseudorotaxane precursor. Dalton Transactions, 2016, 45, 13304-13307.	1.6	17
54	Condition dependence of Zr electrochemical reactions and morphological evolution of Zr deposits in molten salt. Science China Chemistry, 2017, 60, 264-274.	4.2	17

#	Article	IF	CITATIONS
55	Development of picosecond time-resolved X-ray absorption spectroscopy by high-repetition-rate laser pump/X-ray probe at Beijing Synchrotron Radiation Facility. Journal of Synchrotron Radiation, 2017, 24, 667-673.	1.0	17
56	Two novel uranyl complexes of a semi-rigid aromatic tetracarboxylic acid supported by an organic base as an auxiliary ligand or a templating agent: an experimental and theoretical exploration. CrystEngComm, 2015, 17, 3031-3040.	1.3	16
57	High energy and high brightness laser compton backscattering gamma-ray source at IHEP. Matter and Radiation at Extremes, 2018, 3, 219-226.	1.5	16
58	Radiationâ€Induced Selfâ€Assembly of Ti ₃ C ₂ T <i>_x</i> with Improved Electrochemical Performance for Supercapacitor. Advanced Materials Interfaces, 2020, 7, 1901839.	1.9	16
59	Competitive Coordination of Chloride and Fluoride Anions Towards Trivalent Lanthanide Cations (La ³⁺ and Nd ³⁺) in Molten Salts. Chemistry - A European Journal, 2021, 27, 11721-11729.	1.7	16
60	The influence of Fâ ^{^,} ion on the electrochemical behavior and coordination properties of uranium in LiCl-KCl molten salt. Electrochimica Acta, 2022, 404, 139573.	2.6	16
61	Fabrication of nanofluidic diodes with polymer nanopores modified by atomic layer deposition. Biomicrofluidics, 2014, 8, 052111.	1.2	15
62	An Unprecedented Twoâ€Fold Nested Superâ€Polyrotaxane: Sulfateâ€Directed Hierarchical Polythreading Assembly of Uranyl Polyrotaxane Moieties. Chemistry - A European Journal, 2016, 22, 11329-11338.	1.7	15
63	Preparation of γ-Uranium-Molybdenum Alloys by Electrochemical Reduction of Solid Oxides in LiCl Molten Salt. Journal of the Electrochemical Society, 2019, 166, D276-D282.	1.3	15
64	Growth of Uranyl Hydroxide Nanowires and Nanotubes by the Electrodeposition Method and Their Transformation to One-Dimensional U3O8Nanostructures. European Journal of Inorganic Chemistry, 2014, 2014, 1158-1164.	1.0	14
65	Uranium chemical species in LiCl-KCl eutectic under different conditions for the dissolution of U3O8. Journal of Nuclear Materials, 2020, 542, 152475.	1.3	14
66	Electrochemical extraction kinetics of Nd on reactive electrodes. Separation and Purification Technology, 2022, 281, 119853.	3.9	14
67	Interactions between U(VI) and bovine serum albumin. Journal of Radioanalytical and Nuclear Chemistry, 2013, 298, 903-908.	0.7	13
68	Electrodeposition Mechanism of La ³⁺ on Al, Ga and Al-Ga Alloy Cathodes in LiCl-KCl Eutectic Salt. Journal of the Electrochemical Society, 2021, 168, 062511.	1.3	13
69	Non-linear streaming conductance in a single nanopore by addition of surfactants. Applied Physics Letters, 2014, 104, 033108.	1.5	11
70	Incorporation of magnetism into the dihydroimidazole functionalized mesoporous silica for convenient U(VI) capture. Journal of Radioanalytical and Nuclear Chemistry, 2016, 308, 447-458.	0.7	11
71	Thermodynamic properties of praseodymium on the liquid cadmium electrode and evaluation of anodic dissolution behavior in LiCl-KCl eutectic. Journal of Nuclear Materials, 2019, 523, 16-25.	1.3	11
72	Hydrolytically stable foamed HKUST-1@CMC composites realize high-efficient separation of U(VI). IScience, 2021, 24, 102982.	1.9	9

#	Article	IF	CITATIONS
73	Chemical Species Transformation during the Dissolution Process of U ₃ O ₈ and UO ₃ in the LiCl–KCl–AlCl ₃ Molten Salt. Inorganic Chemistry, 2022, 61, 6519-6529.	1.9	9
74	Low-voltage electroosmotic pumping using polyethylene terephthalate track-etched membrane. Nuclear Instruments & Methods in Physics Research B, 2012, 286, 223-228.	0.6	8
75	Three-dimensional polyaniline architecture enabled by hydroxyl-terminated Ti ₃ C ₂ T _{<i>x</i>/sub> MXene for high-performance supercapacitor electrodes. Materials Chemistry Frontiers, 2021, 5, 7883-7891.}	3.2	8
76	Separation of uranium from lanthanides (La, Sm) with sacrificial Li anode in LiCl-KCl eutectic salt. Separation and Purification Technology, 2022, 292, 121025.	3.9	8
77	Nanofluidic Pulser Based on Polymer Conical Nanopores. Journal of Physical Chemistry C, 2011, 115, 22736-22741.	1.5	7
78	Synthesis of ordered mesoporous uranium dioxide by a nanocasting route. Radiochimica Acta, 2016, 104, 549-553.	0.5	6
79	Thorium(IV) adsorption onto multilayered Ti ₃ C ₂ T _x MXene: a batch, X-ray diffraction and EXAFS combined study. Journal of Synchrotron Radiation, 2021, 28, 1709-1719.	1.0	4
80	Progress on the construction of the 100 MeV/100 kW electron linac for the NSC KIPT neutron source. Chinese Physics C, 2014, 38, 047005.	1.5	3
81	Synthesis of ordered mesoporous U ₃ O ₈ by a nanocasting route. Radiochimica Acta, 2014, 102, 813-816.	0.5	3
82	Uranyl-containing heterometallic coordination polymers based on 4-(4'-carboxyphenyl)-1,2,4-triazole ligand: structure regulation through subtle changes of the secondary metal centers. Journal of Coordination Chemistry, 2018, 71, 3021-3033.	0.8	3
83	Ionic current conduction at low voltage of track-etched double conical nanopores modified by surfactant CTAB. Journal of Polymer Research, 2020, 27, 1.	1.2	1
84	Two-dimensional transition metal carbide/nitride (MXene)-based nanomaterials for removal of toxic/radioactive metal ions from wastewater. , 2022, , 161-194.		0